TIME-DOMAIN CHANNEL ESTIMATION FOR WIDEBAND MILLIMETER WAVE SYSTEMS WITH HYBRID ARCHITECTURE

Kiran Venugopal[†], *Ahmed Alkhateeb*[†], *Robert W. Heath, Jr.*[†] *and Nuria González Prelcic* [‡]

[†]The University of Texas, Austin, TX, USA, Email: {kiranv, aalkhateeb, rheath}@utexas.edu
[‡]The University of Vigo, Spain, Email: nuria@gts.uvigo.es

ABSTRACT

Millimeter wave (mmWave) systems will likely employ large antennas at both the transmitter and receiver for directional beamforming. Hybrid analog/digital MIMO architectures have been proposed previously for leveraging both array gain and multiplexing gain, while reducing the power consumption in analog-to-digital converters. Channel knowledge is needed to design the hybrid precoders/combiners, which is difficult to obtain due to the large antenna arrays and the frequency selective nature of the channel. In this paper, we propose a sparse recovery based time-domain channel estimation technique for hybrid architecture based frequency selective mmWave systems. The proposed compressed sensing channel estimation algorithm is shown to require much less training overhead compared to the existing protocol, while also providing the explicit estimation of the channel. The results show that using multiple RF chains at the receiver and the transmitter further reduces the training overhead.

***Index Terms*—** Millimeter wave communication, channel estimation, hybrid architecture, compressed sensing

1. INTRODUCTION

Millimeter wave (mmWave) based communication is a key ingredient of 5G wireless systems for realizing Gbps data rates [1–4]. To provide sufficient received signal power in mmWave systems, large antenna arrays need to be deployed at both the transmitter and the receiver [3,5]. Developing low-overhead mmWave channel estimation techniques is crucial for acquiring channel state information used to design precoding matrices in mulit-user mmWave MIMO systems [6]. This is, however, complicated due to hardware constraints and low signal-to-noise-ratios (SNR) without beamforming in the antenna front-end [7].

Analog beam training is a solution proposed previously to iteratively find the best beamforming vectors at the transceivers to maximize link SNR [8,9]. While analog beam training works for both narrowband and wideband systems, the downside is that the solution supports only a single communication stream. Additionally, larger training overhead is incurred for finer beam training and in multi-user systems. Fully digital channel estimation is infeasible because of the resulting high power consumption in mixed signal components, and the potential under-utilization of array gains necessary for meeting link budget. Channel estimation and precoding using hybrid architectures, that leverage both array gain and multiplexing gain in large antenna mmWave systems have been studied in [6,10,11]. Hybrid solutions in mmWave communication can also support multi-user systems thanks to the the extra signal processing in the baseband. Prior work considered mainly narrowband mmWave systems, while in practice, mmWave channels will be wideband and frequency selective. In [12], hybrid precoding for frequency selective mmWave systems was studied, though the channel estimation techniques were not elaborated, especially for single-carrier modulation which is a promising solution for mmWave [13].

In this paper, we propose a time-domain wideband channel estimation technique for mmWave systems using hybrid architecture. The proposed approach simultaneously leverages the structure in the frequency selective large antenna mmWave channel, and the power and cost saving advantages of employing hybrid solutions at the transceivers. Moreover, the proposed channel estimation technique can be used to enable MIMO and multi-user communication in 802.11ad, as a potential application area. One of the primary foci of the paper is to formulate the wideband channel estimation in large antenna systems as a sparse recovery problem while considering the hardware constraints relevant for mmWave communication systems. It is shown through simulation results that the proposed algorithm requires significantly less training steps to reliably estimate the channel by utilizing multiple RF chains at the transceivers.

Notation: Bold uppercase $\mathbf{A}$, bold lower case $\mathbf{a}$ and non-bold lower case a are used to denote matrices, column vectors and scalar values, respectively. We use $\mathcal{A}$ to denote a set. Further, $||\mathbf{A}||_F$ is the Frobenius norm, and $\mathbf{A}^*$, $\bar{\mathbf{A}}$ and $\mathbf{A}^T$ are the conjugate transpose, conjugate, and transpose of the matrix $\mathbf{A}$. The (i, j)th entry of matrix $\mathbf{A}$ is denoted using $[\mathbf{A}]_{i,j}$. If $\mathbf{A}$ and $\mathbf{B}$ are two matrices, $\mathbf{A} \circ \mathbf{B}$ is the Khatri-Rao product of $\mathbf{A}$ and $\mathbf{B}$, and $\mathbf{A} \otimes \mathbf{B}$ is their Kronecker product.

This work was supported in part by the Intel-Verizon 5G research program and the National Science Foundation under Grant No. NSF-CCF-1319556.

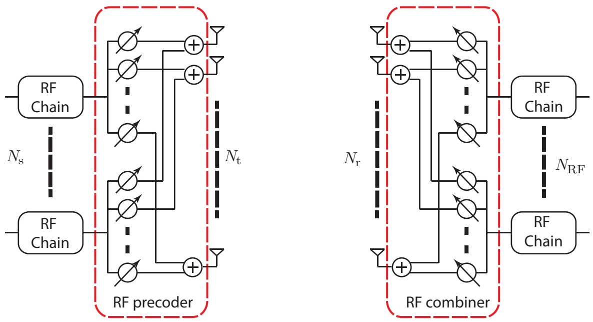

Fig. 1. Figure illustrating the transmitter and receiver structure assumed in the paper. The RF precoder and the combiner are implemented using a network of phase shifters.

2. SYSTEM MODEL

Consider a single-user mmWave MIMO system with a transmitter having N_t antennas and a receiver with N_r antennas. Both the transmitter and the receiver are assumed to have N_RF RF chains as shown in Fig. 1. The transmitter uses a hybrid precoder [12, 14] $\mathbf{F} = \mathbf{F}_\mathrm{RF}\mathbf{F}_\mathrm{BB} \in \mathbb{C}^{N_\mathrm{t} \times N_\mathrm{s}}$, N_s being the number of data streams that can be transmitted. Denoting the symbol vector at instance n as $\mathbf{s}_n \in \mathbb{C}^{N_\mathrm{s} \times 1}$, satisfying $\mathbb{E}[\mathbf{s}_n\mathbf{s}_n^*] = \frac{1}{N_\mathrm{s}}\mathbf{I}$, the signal transmitted at discrete-time n is $\tilde{\mathbf{s}}_n = \mathbf{F}\mathbf{s}_n$.

The $N_\mathrm{r} \times N_\mathrm{t}$ channel matrix between the transmitter and the receiver is assumed to be frequency selective, having a delay tap length N_c and is denoted as $\mathbf{H}_d,\ d = 0,\ 2,\ \ldots,\ N_\mathrm{c} - 1$. With ρ denoting the average received power and $\mathbf{v}_n \sim \mathcal{N}\left(0, \sigma^2\mathbf{I}\right)$ denoting the circularly symmetric complex Gaussian distributed additive noise vector, the received signal can be written as

$$\mathbf{r}_n \quad = \quad \sqrt{\rho}\sum_{d=0}^{N_\mathrm{c}-1}\mathbf{H}_d\mathbf{F}\mathbf{s}_{n-d} + \mathbf{v}_n. \qquad (1)$$

The receiver applies a hybrid combiner $\mathbf{W} = \mathbf{W}_\mathrm{RF}\mathbf{W}_\mathrm{BB} \in \mathbb{C}^{N_\mathrm{r} \times N_\mathrm{RF}}$ so that the post combining signal at the receiver is

$$\mathbf{y}_n = \sqrt{\rho}\sum_{d=0}^{N_\mathrm{c}-1}\mathbf{W}^*\mathbf{H}_d\mathbf{F}\mathbf{s}_{n-d} + \mathbf{W}^*\mathbf{v}_n. \qquad (2)$$

There are several RF precoder and combiner architectures that can be implemented [11]. In this paper, we assume a fully connected phase shifting network [11, A1]. We assume a hardware constraint that only the quantized angles in the set

$$\mathcal{A} = \left\{0,\ \frac{2\pi}{2^{N_\mathrm{Q}}},\ \cdots,\ \frac{\left(2^{N_\mathrm{Q}} - 1\right)2\pi}{2^{N_\mathrm{Q}}}\right\} \qquad (3)$$

can be realized in the phase shifters. Here, N_Q is the number of angle quantization bits. This implies $[\mathbf{F}]_{i,j} = \frac{1}{\sqrt{N_\mathrm{t}}}e^{\mathrm{j}\varphi_{i,j}}$ and $[\mathbf{W}]_{i,j} = \frac{1}{\sqrt{N_\mathrm{r}}}e^{\mathrm{j}\omega_{i,j}}$, with $\varphi_{i,j},\ \omega_{i,j} \in \mathcal{A}$.

3. CHANNEL ESTIMATION VIA COMPRESSED SENSING

In this section, we present our proposed explicit channel estimation algorithm that leverages the sparse wideband mmWave channel.

3.1. Frequency Selective Channel Model

Consider a geometric channel model [10, 15] for the frequency selective mmWave channel consisting of L scattering clusters. The dth delay tap of the channel can be expressed as

$$\mathbf{H}_d \quad = \quad \sqrt{\frac{N_\mathrm{r}N_\mathrm{t}}{L}}\sum_{\ell=1}^{L}\alpha_\ell p_\mathrm{rc}(dT_s - \tau_\ell)\mathbf{a}_\mathrm{R}(\phi_\ell)\mathbf{a}_\mathrm{T}^*(\theta_\ell), \qquad (4)$$

where $p_\mathrm{rc}(\tau)$ denotes the raised cosine pulse signal evaluated at τ, $\alpha_\ell \in \mathbb{C}$ is the complex gain of the ℓth cluster, $\tau_\ell \in \mathbb{R}$ is the delay of the ℓth cluster, $\phi_\ell \in [0, 2\pi)$ and $\theta_\ell \in [0, 2\pi)$ are the angles of arrival and departure (AoA/AoD), respectively of the ℓth cluster, and $\mathbf{a}_\mathrm{R}(\phi_\ell) \in \mathbb{C}^{N_\mathrm{r} \times 1}$ and $\mathbf{a}_\mathrm{T}(\theta_\ell) \in \mathbb{C}^{N_\mathrm{t} \times 1}$ denote the antenna array response vectors of the receiver and transmitter, respectively.

The channel model in (4) can be written compactly as

$$\mathbf{H}_d \quad = \quad \mathbf{A}_\mathrm{R}\boldsymbol{\Delta}_d\mathbf{A}_\mathrm{T}^*, \qquad (5)$$

where $\boldsymbol{\Delta}_d \in \mathbb{C}^{L \times L}$ is diagonal with non-zero complex entries, and $\mathbf{A}_\mathrm{R} \in \mathbb{C}^{N_\mathrm{r} \times L}$ and $\mathbf{A}_\mathrm{T} \in \mathbb{C}^{N_\mathrm{t} \times L}$ contain the columns $\mathbf{a}_\mathrm{R}(\phi_\ell)$ and $\mathbf{a}_\mathrm{T}(\theta_\ell)$, respectively. Under this notation, vectorizing the channel matrix in (5) gives

$$vec(\mathbf{H}_d) = \sqrt{\frac{N_\mathrm{t}N_\mathrm{t}}{L}}\left(\bar{\mathbf{A}}_\mathrm{T} \circ \mathbf{A}_\mathrm{R}\right)\begin{bmatrix}\alpha_1 p_\mathrm{rc}(dT_s - \tau_1)\\ \alpha_2 p_\mathrm{rc}(dT_s - \tau_2)\\ \vdots\\ \alpha_L p_\mathrm{rc}(dT_s - \tau_L)\end{bmatrix}. \qquad (6)$$

Note that the ℓth column of $\bar{\mathbf{A}}_\mathrm{T} \circ \mathbf{A}_\mathrm{R}$ is of the form $\bar{\mathbf{a}}_\mathrm{T}(\theta_\ell) \otimes \mathbf{a}_\mathrm{R}(\phi_\ell)$.

3.2. Sparse Formulation

We assume block transmission with zero padding (ZP) appended to each transmitted frame and hybrid architecture at the transmitter and the receiver. To formulate the sparse recovery problem, we assume single RF chains are used both the transmitter and the receiver for the ease of exposition. The formulation extends directly for multiple RF chains at the transmitter and the receiver. Accordingly, for the mth training frame the transmitter uses an RF precoder $\mathbf{f}_m$ that can be realized using quantized angles at the analog phase shifters. The nth symbol of the mth received frame is

$$\mathbf{r}_n^{(m)} \quad = \quad \sqrt{\rho}\sum_{d=0}^{N_\mathrm{c}-1}\mathbf{H}_d\mathbf{f}_m s_{n-d}^{(m)} + \mathbf{v}_n^{(m)}, \qquad (7)$$

where $s_n^{(m)}$ is the nth non-zero symbol of the mth training frame of length $N+N_\mathrm{c}-1$

$$\mathbf{s}^{(m)} = [\,\underbrace{0 \cdots 0}_{N_\mathrm{c}-1}\; s_1^{(m)} \;\cdots\; s_N^{(m)}\,]. \quad (8)$$

At the receiver, an RF combiner $\mathbf{w}_m$ is used during the mth training phase, so that the post combining signal is

$$\begin{bmatrix} y_1^{(m)} \\ y_2^{(m)} \\ \vdots \\ y_N^{(m)} \end{bmatrix}^T = \sqrt{\rho}\mathbf{w}_m^*\left[\mathbf{H}_0 \cdots \mathbf{H}_{N_\mathrm{c}-1}\right]\mathbf{S}^{(m)T} \otimes \mathbf{f}_m + \mathbf{e}^{(m)T}, \quad (9)$$

$$\text{where } \mathbf{S}^{(m)} = \begin{bmatrix} s_1^{(m)} & 0 & \cdots & 0 \\ s_2^{(m)} & s_1^{(m)} & \cdots & . \\ \vdots & \vdots & \ddots & \vdots \\ s_N^{(m)} & \cdots & \cdots & s_{N-N_\mathrm{c}+1}^{(m)} \end{bmatrix}. \quad (10)$$

The use of block transmission with $N_\mathrm{c}-1$ zero padding is important here, since it would allow for reconfiguring the RF circuits from one frame to the other and avoids loss of training data during this reconfiguration. This would also avoid inter frame interference. Also note that for high symboling rates in mmWave systems (the chip rate used in IEEE 802.11ad preamble, for example, is 1760 MHZ), it is impractical to use different precoders and combiners for different symbols. It is more feasible, however, to change the RF circuitry for different frames. Vectorizing (9) gives

$$\mathbf{y}^{(m)} = \sqrt{\rho}\mathbf{S}^{(m)} \otimes \mathbf{f}_m^T \otimes \mathbf{w}_m^* \begin{bmatrix} vec(\mathbf{H}_0) \\ vec(\mathbf{H}_1) \\ \vdots \\ vec(\mathbf{H}_{N_\mathrm{c}-1}) \end{bmatrix} + \mathbf{e}^{(m)}. \quad (11)$$

To formulate the compressed sensing problem we first exploit the sparse nature of the channel in the angular domain. Assuming the AoAs and AoDs are drawn from an angle grid on G_r and G_t, respectively and neglecting the grid quantization error, we can then express (11) as

$$\mathbf{y}^{(m)} = \sqrt{\rho}\left(\mathbf{S}^{(m)} \otimes \mathbf{f}_m^T \otimes \mathbf{w}_m^*\right)\left(\mathbf{I}_{N_\mathrm{c}} \otimes \bar{\mathbf{A}}_\mathrm{tx} \otimes \mathbf{A}_\mathrm{rx}\right)\hat{\mathbf{x}} + \mathbf{e}^{(m)}, \quad (12)$$

where $\mathbf{A}_\mathrm{tx}$ and $\mathbf{A}_\mathrm{rx}$ are the dictionary matrices used for sparse recovery. The $N_\mathrm{t} \times G_\mathrm{t}$ matrix $\mathbf{A}_\mathrm{tx}$ consists of columns $\mathbf{a}_\mathrm{T}(\tilde{\theta}_x)$, with $\tilde{\theta}_x$ drawn from a quantized angle grid of size G_t, and the $N_\mathrm{r} \times G_\mathrm{r}$ matrix $\mathbf{A}_\mathrm{rx}$ consists of columns $\mathbf{a}_\mathrm{R}(\tilde{\phi}_x)$, with $\tilde{\phi}_x$ drawn from a quantized angle grid of size G_r. The signal $\hat{\mathbf{x}}$ consists of the channel gains and pulse shaping filter response, and is of size $N_\mathrm{c}G_\mathrm{r}G_\mathrm{t} \times 1$.

Next, the band-limited nature of the sampled pulse shaping filter is used to make the measurement vector more sparse. Define

$$p_n(\tau) = p_\mathrm{rc}(n-\tau) \quad (13)$$

$$\text{and } \Delta_{ps}(n) = diag\left([p_n(\tau_1)\; p_n(\tau_2) \;\cdots\; p_n(\tau_L)]\right). \quad (14)$$

Using (13) and (14), (6) can be written as

$$vec(\mathbf{H}_d) = \sqrt{\frac{N_\mathrm{t}N_\mathrm{t}}{L}}\left(\bar{\mathbf{A}}_\mathrm{T} \circ \mathbf{A}_\mathrm{R}\right)\Delta_{ps}(dT_s)\begin{bmatrix} \alpha_1 \\ \alpha_2 \\ \vdots \\ \alpha_L \end{bmatrix}. \quad (15)$$

Next, we look at the sampled version of the pulse-shaping filter $\tilde{\mathbf{p}}_n$ having entries $\tilde{p}_n(k)$, for $n = 1, 2, \cdots, N_\mathrm{c}$ and $k = 1, 2, \cdots, G_\mathrm{c}$. Then, neglecting the quantization error due to sampling in the delay domain, and combining (11), (12), and (15) we can write (12) as

$$\mathbf{y}^{(m)} = \sqrt{\rho}\left(\mathbf{S}^{(m)} \otimes \mathbf{f}_m^T \otimes \mathbf{w}_m^*\right)\left(\mathbf{I}_{N_\mathrm{c}} \otimes \bar{\mathbf{A}}_\mathrm{tx} \otimes \mathbf{A}_\mathrm{rx}\right)\mathbf{\Gamma}\mathbf{x} + \mathbf{e}^{(m)},$$

$$\text{where} \quad \mathbf{\Gamma} = \begin{bmatrix} \mathbf{I}_{G_\mathrm{r}G_\mathrm{t}} \otimes \tilde{\mathbf{p}}_1^T \\ \mathbf{I}_{G_\mathrm{r}G_\mathrm{t}} \otimes \tilde{\mathbf{p}}_2^T \\ \vdots \\ \mathbf{I}_{G_\mathrm{r}G_\mathrm{t}} \otimes \tilde{\mathbf{p}}_{N_\mathrm{c}}^T \end{bmatrix},$$

and $\mathbf{x}$ is $G_\mathrm{c}G_\mathrm{r}G_\mathrm{t} \times 1$ sparse vector containing the complex channel gains.

Stacking M such measurements obtained from sending M training frames using different RF precoder and combiner for each frame, we have

$$\mathbf{y} = \sqrt{\rho}\mathbf{\Phi}\mathbf{\Psi}\mathbf{x} + \mathbf{e}, \quad (16)$$

where $\mathbf{y} = \left[\mathbf{y}^{(1)}, \mathbf{y}^{(2)}, ..., \mathbf{y}^{(M)}\right]^T \in \mathbb{C}^{NM \times 1}$ is the measured signal,

$$\mathbf{\Phi} = \begin{bmatrix} \mathbf{S}^{(1)} \otimes \mathbf{f}_1^T \otimes \mathbf{w}_1^* \\ \mathbf{S}^{(2)} \otimes \mathbf{f}_2^T \otimes \mathbf{w}_2^* \\ \vdots \\ \mathbf{S}^{(M)} \otimes \mathbf{f}_M^T \otimes \mathbf{w}_M^* \end{bmatrix} \in \mathbb{C}^{NM \times N_\mathrm{c}N_\mathrm{r}N_\mathrm{t}} \quad (17)$$

is the measurement matrix, and

$$\mathbf{\Psi} = \left(\mathbf{I}_{N_\mathrm{c}} \otimes \bar{\mathbf{A}}_\mathrm{tx} \otimes \mathbf{A}_\mathrm{rx}\right)\mathbf{\Gamma} \quad (18)$$

$$= \begin{bmatrix} \left(\bar{\mathbf{A}}_\mathrm{tx} \otimes \mathbf{A}_\mathrm{rx}\right) \otimes \tilde{\mathbf{p}}_1^T \\ \left(\bar{\mathbf{A}}_\mathrm{tx} \otimes \mathbf{A}_\mathrm{rx}\right) \otimes \tilde{\mathbf{p}}_2^T \\ \vdots \\ \left(\bar{\mathbf{A}}_\mathrm{tx} \otimes \mathbf{A}_\mathrm{rx}\right) \otimes \tilde{\mathbf{p}}_{N_\mathrm{c}}^T \end{bmatrix} \in \mathbb{C}^{N_\mathrm{c}N_\mathrm{r}N_\mathrm{t} \times G_\mathrm{c}G_\mathrm{r}G_\mathrm{t}} \quad (19)$$

is the dictionary. The beamforming and combining vectors $\mathbf{f}_m, \mathbf{w}_m, m = 1, 2, \cdots, M$ used for training have the phase angles chosen uniformly at random from the set $\mathcal{A}$ in (3).

AoA/AoD estimation With the sparse formulation of the mmWave channel estimation problem in (16), compressed sensing tools can be first used to estimate the AoA and AoD. Note that we can increase or decrease G_r, G_t and G_c to meet the required level of sparsity. As the sensing matrix is known at the receiver, sparse recovery algorithms can be used to estimate the AoA and AoD. Following this, the channel gains can be estimated to minimize the minimum mean squared error or via least squares by plugging in the columns of the dictionary matrices corresponding to the estimated AoA and AoD.

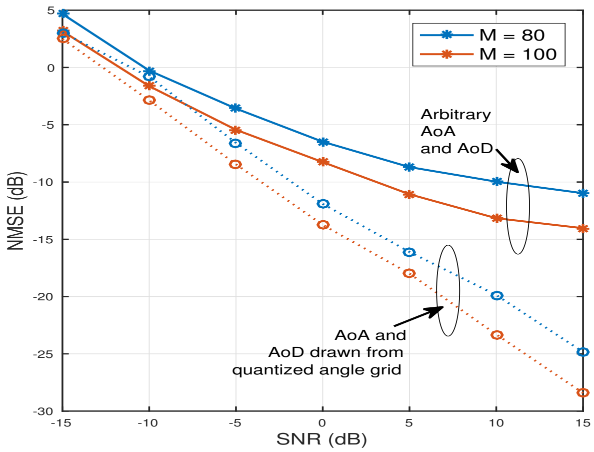

Fig. 2. Normalized mean squared error (NMSE) as a function of SNR for different training length M when $N_s = 1$ and $N_{\text{RF}} = 1$.Using the proposed approach, training length of $80 - 100$ is sufficient to ensure very low estimation error

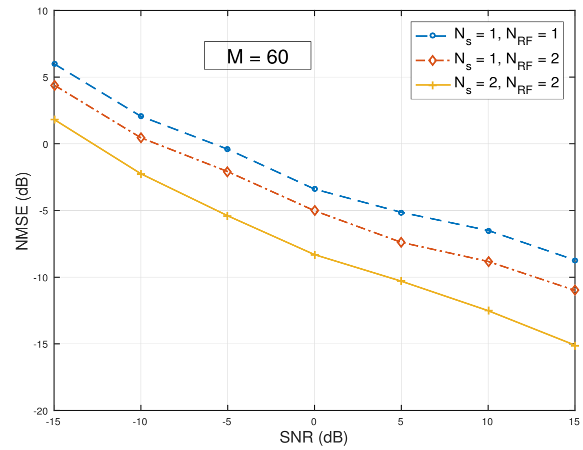

Fig. 3. NMSE as a function of SNR for different numbers of RF combiners N_{RF} used at the receiver and different number of transmit streams N_s.

4. SIMULATION RESULTS

In this section, the performance of the proposed channel estimation algorithm is provided. For the compressed sensing estimation of the angles of arrival and departure, compressive sampling matching pursuit [16] is used. The channel gains are then estimated using least squares.

We consider a system with $N_{\text{t}} = 32$ transmitter antennas and $N_{\text{r}} = 32$ receiver antennas for illustration. Uniform linear array with half wavelength separation are assumed. The AoA and AoD quantization used for construction of the transmitter and receiver dictionary matrices are taken to be $G_{\text{r}} = 64$ and $G_{\text{t}} = 64$, respectively. The angle quantization used in the phase shifters is assumed to have $N_{\text{Q}} = 2$ quantization bits so that the entries of $\mathbf{f}_m, \ \mathbf{w}_m, m = 1, \ 2, \ \cdots, \ M$ are drawn from $\{1, \ -1, \ \text{j}, \ -\text{j}\}$ with equal probability. The frame length is assumed to be $N = 16$ and the delay tap length of the frequency selective channel is assumed to be $N_{\text{c}} = 4$ for illustration. The raised cosine pulse shaping signal is assumed to have a roll-off factor of 0.8.

Fig. 2 shows the normalized mean squared error (NMSE) of the channel estimates as a function of the post combining received signal SNR. Here we define NMSE as

$$\texttt{NMSE} = \frac{\sum_{d=0}^{N_{\text{c}}} ||\mathbf{H}_d - \hat{\mathbf{H}}_d||_F^2}{\sum_{d=0}^{N_{\text{c}}} ||\mathbf{H}_d||_F^2} \tag{20}$$

for comparing the effectiveness of our proposed channel estimation algorithm. From Fig. 2, it can be seen that with training length of even $80 - 100$ frames, sufficiently low channel estimation error can be ensured. For comparing the impact of angle quantization error, we show the NMSE for the case when the AoAs/AoDs are drawn from quantized grids and also the case when the AoAs/AoDs are unrestricted. Choosing larger values for G_{r} (G_{t}) in comparison with N_{r} (N_{t}) can further narrow the error gap between the two cases.

Fig. 3 shows how employing multiple RF chains at the transmitter and receiver can give good improvement in the estimation performance while requiring fewer number of training frame transmissions. In Fig. 3, we assume $M = 60$ frames are transmitted for training. The improvement in performance occurs thanks to a larger number of effective measurements per training sent, that scales with the number of RF combiners N_{RF} at the receiver. Similarly, employing multiple streams N_s at the transmitter contributes to a larger set of random precoders, resulting in smaller estimation error via compressed sensing. So, larger N_{RF} and N_s are preferred to decrease the training overhead and to fully leverage the hybrid architecture in wideband mmWave systems.

5. CONCLUSION

In this paper, we proposed a time-domain channel estimation algorithm for frequency selective mmWave systems using hybrid architecture at the transmitter and receiver. The proposed channel training protocol is backward compatible with the preamble structure used in IEEE 802.11ad and can support MIMO operation since the entire channel is estimated after the beam training phase. Simulation results showed that the proposed algorithm required very few training frames to ensure low estimation error, and further reduction can be obtained by employing multiple RF chains at the transmitter and the receiver.

6. REFERENCES

[1] F. Boccardi *et al*, “Five disruptive technology directions for 5G,” *IEEE Commun. Mag.*, vol. 52, pp. 74–80, Feb. 2014.

[2] J. Andrews *et al*, “What will 5G be?,” *IEEE J. Sel. Areas Commun.*, vol. 32, pp. 1065–1082, June 2014.

[3] Z. Pi and F. Khan, “An introduction to millimeter-wave mobile broadband systems,” *IEEE Commun. Mag.*, vol. 49, pp. 101–107, June 2011.

[4] T. Rappaport *et al*, “Millimeter wave mobile communications for 5G cellular: It will work!,” *IEEE Access*, vol. 1, pp. 335–349, May 2013.

[5] W. Roh *et al*, “Millimeter-wave beamforming as an enabling technology for 5G cellular communications: theoretical feasibility and prototype results,” *IEEE Commun. Mag.*, vol. 52, pp. 106–113, Feb 2014.

[6] A. Alkhateeb, G. Leus, and R. W. Heath, “Compressed sensing based multi-user millimeter wave systems: How many measurements are needed?,” in *Proc. IEEE Int. Conf. Acoustics, Speech and Sig. Process. (ICASSP)*, pp. 2909–2913, April 2015.

[7] R. W. Heath, N. Gonzlez-Prelcic, S. Rangan, W. Roh, and A. M. Sayeed, “An overview of signal processing techniques for millimeter wave MIMO systems,” *IEEE J. Sel. Areas Commun.*, vol. 10, pp. 436–453, April 2016.

[8] J. Wang, “Beam codebook based beamforming protocol for multi-Gbps millimeter-wave WPAN systems,” *IEEE J. Sel. Areas Commun.*, vol. 27, pp. 1390–1399, Oct 2009.

[9] S. Hur, T. Kim, D. J. Love, J. V. Krogmeier, T. A. Thomas, and A. Ghosh, “Millimeter wave beamforming for wireless backhaul and access in small cell networks,” *IEEE Trans. Commun.*, vol. 61, pp. 4391–4403, October 2013.

[10] A. Alkhateeb, O. E. Ayach, G. Leus, and R. W. Heath Jr., “Channel estimation and hybrid precoding for millimeter wave cellular systems,” *IEEE J. Sel. Topics Signal Process.*, vol. 8, pp. 831–846, Oct 2014.

[11] R. M. Rial, C. Rusu, A. Alkhateeb, N. G. Prelcic, and R. W. Heath Jr., “Hybrid MIMO architectures for millimeter wave communications: Phase shifters or switches?,” *IEEE Access*, Jan 2016.

[12] A. Alkhateeb and R. W. Heath Jr., “Frequency selective hybrid precoding for limited feedback millimeter wave systems,” *IEEE Trans. Commun.*, vol. 64, pp. 1801–1818, May 2016.

[13] A. Ghosh *et al*, “Millimeter-wave enhanced local area systems: A high-data-rate approach for future wireless networks,” *IEEE J. Sel. Areas Commun.*, vol. 32, pp. 1152–1163, June 2014.

[14] O. E. Ayach, S. Rajagopal, S. Abu-Surra, Z. Pi, and R. W. Heath Jr., “Spatially sparse precoding in millimeter wave MIMO systems,” *IEEE Trans. Commun.*, vol. 13, pp. 1499–1513, Mar. 2014.

[15] P. Schniter and A. Sayeed, “Channel estimation and precoder design for millimeter-wave communications: The sparse way,” in *Proc. Asilomar Conf. Signals, Syst., Comput.*, pp. 273–277, Nov 2014.

[16] D. Needell and J. A. Tropp, “CoSaMP: Iterative signal recovery from incomplete and inaccurate samples,” *Applied and Computational Harmonic Analysis*, vol. 26, no. 3, pp. 301–321, 2009.